Microscale observations of sulfate reduction: Correlation of microbial activity with lithified micritic laminae in modern marine stromatolites

Pieter T. Visscher* Department of Marine Sciences, University of Connecticut, Groton, Connecticut 06340, USA
R. Pamela Reid Rosenstiel School of Marine and Atmospheric Science, University of Miami, Miami, Florida 33149, USA
Brad M. Bebout NASA Ames Research Center, Moffett Field, California 94035, USA

ABSTRACT

We report for the first time micrometer-scale correlation of geologic and microbial processes in modern marine stromatolites. Precipitation of micritic laminae in these stromatolites was studied by comparing microstructure, as observed in petrographic thin sections, with microbial sulfate-reduction activity. Two-dimensional mapping of sulfate-reduction rates was implemented by incubating a vertical section of a stromatolite face on silver foil coated with $^{35}SO_4^{2-}$. Our results show that sulfate-reduction activity is high in zones of $CaCO_3$ precipitation and indicate that microbial activity produces lithified micritic laminae near the surface of the stromatolites. Similarities with micritic laminae in ancient stromatolites suggest that sulfate reduction may also have been an important mechanism of carbonate precipitation in these fossilized structures.

Keywords: stromatolites, calcium carbonate precipitation, sulfate reduction, bacteria.

INTRODUCTION

Modern marine stromatolites, found in the Exuma Cays, Bahamas (Dill et al., 1986; Reid et al., 1995), are laminated lithified structures that are formed by microbial activity near their surfaces (Reid et al., 1995; Golubic and Browne, 1996; Macintyre et al., 1996; Feldmann and Mackenzie, 1998). Study of these modern stromatolites extends the knowledge of biologically mediated precipitation, which could have been important in the formation of ancient counterparts. Microbial mats in intertidal and extreme environments have been studied as analogues to enhance understanding of geomicrobiological processes in stromatolites (Des Marais, 1990). However, a major difference between these mats and microbial mats forming stromatolites is that the latter contain lithified laminae of microcrystalline carbonate (micrite) and form characteristic domal or columnar structures. Furthermore, although microbial ecology of intertidal mat development has been described in detail (Van Gemerden, 1993), biogeochemical processes of stromatolite formation in mineralizing mat systems are poorly known. Consequently, biotic versus abiotic origins of ancient stromatolitic deposits remain a subject of controversy (Grotzinger and Knoll, 1999).

Microbial activity mediates precipitation and dissolution of $CaCO_3$ (Krumbein et al., 1977; Froelich et al., 1979; Walter et al., 1993; Kempe and Kazmierczak, 1994). Sulfate reduction has long been linked to $CaCO_3$ precipitation (Baas Becking, 1934; Abd-El-Malek and Rizk, 1963). Sulfate-reducing bacteria have been suggested to mediate carbonate precipitation in microbial mats (Jørgensen and Cohen, 1977; Lyons et al., 1984; Buczynski and Chafetz, 1991; Visscher et al., 1998), and other sedimentary deposits (Froelich et al., 1979; Kazmierczak and Kempe, 1990; Thompson and Ferris, 1990; Walter et al., 1993; Vasconcelos et al., 1995). Sulfate is used as an alternative to O_2 in anaerobic microbial respiration. The process of sulfate reduction mediates $CaCO_3$ precipitation according to the following reaction:

$$2[CH_2O] + SO_4^{2-} + Ca^{2+} \rightarrow CaCO_3 + CO_2 + HS^- + H^+ + H_2O,$$

where $[CH_2O]$ indicates organic carbon (e.g., Walter et al., 1993; Visscher et al., 1998). Visscher et al. (1998) measured sulfate reduction in modern marine stromatolites by using traditional $^{35}SO_4^{2-}$ incubations and found increased rates in lithified layers. In addition, these lithified layers contained higher populations of sulfate-reducing bacteria than unlithified layers (Visscher et al., 1998, 1999). Given these observations, it was not surprising that 49%–63% of the total organic carbon in the stromatolitic mats was calculated to be mineralized through sulfate reduction (Visscher et al., 1998). Clearly, this type of microbial activity plays an important role within the stromatolite mat community. The former studies allowed investigation of microbial activity in stromatolites on a millimeter scale; smaller features could not be observed. We were therefore unable to assess the role of sulfate reduction in the formation of micritic laminae <100 μm thick, which are common within the stromatolitic mats (Reid et al., 1995; Macintyre et al., 1996). Here we present the first study in which a two-dimensional distribution of sulfate reduction is mapped on a microscale and compared with petrographic thin sections from the same location within the stromatolitic mats. This methodology enables a direct correlation between geologic microstructure and microbial activity.

*E-mail: pieter.visscher@uconn.edu.

MATERIALS AND METHODS

Sample Description

Samples of microbial mats from subtidal stromatolites (NS8a2 and NS11a) on Highborne Cay, Exuma Cays, Bahamas, were collected in August 1998. A detailed description of the site was published previously (Reid et al., 1999). The stromatolites consist predominantly of fine carbonate sand that is trapped and bound by filaments of the cyanobacterium *Schizothrix* sp. in surficial microbial mats. The cyanobacterial community produces copious amounts of exopolymer (Decho, 1990; Golubic and Browne, 1996). Periodic episodes of lithification within these mats form micritic horizons, which are responsible for the laminated fabric of the stromatolite (Fig. 1A; Reid et al., 1995, 1999; Macintyre et al., 1996).

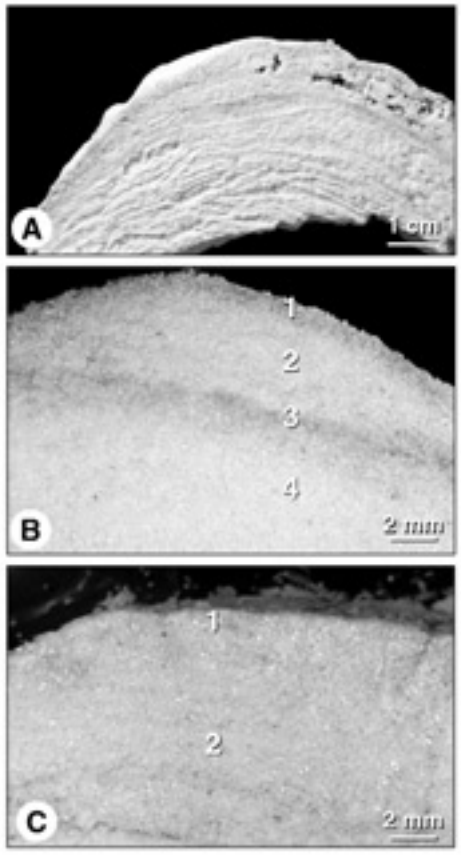

Figure 1. A: Stromatolite from Highborne Cay, Bahamas; lithified layers stand out in relief on cut surface. B and C: Photomicrographs of mat sample NS8a2 (B) and NS11a (C); numbers indicate layers described in text.

Mat samples collected for this study were sawed vertically and photographed; one half of each sample was used for biogeochemical measurements; the matching face, i.e., the other half of the sample, was embedded with epoxy for petrographic thin sectioning. Four layers were identified in sample NS8a2 (Fig. 1B): layer 1, about 0.5 mm thick, is caramel colored and soft; layer 2, 2–3 mm thick, is white and soft; layer 3, 1 mm thick, is gray and crusty; layer 4, 3–4 mm thick, is white and soft. Sample NS11a shows no distinct layers; however, for the purpose of biogeochemical analyses, the top 0.5 mm of the mat was designated as layer 1; depths from 0.5 to 10 mm were designated as layer 2 (Fig. 1C).

Biogeochemical Measurements

Two-dimensional measurement of sulfate reduction activity in NS8a2 and NS11a were made by using $^{35}SO_4^{2-}$-coated silver foil and a modification of the method developed by Cohen (1984; Cohen and Helman, 1997). Strips of Ag foil (20 × 50 mm and 0.1 mm thick; Sigma Chemical Co., St. Louis, Missouri) were treated with acetone, rinsed with water, and coated with a solution of $^{35}SO_4^{2-}$ (1 mCi per foil; Ammersham, Chicago, Illinois) prepared in sterilized seawater from the site. The foil was then allowed to air dry for 24 h. A freshly cut sample of each mat was placed on the silver foil, and, after an incubation time of 6–8 h in the dark, the sample was removed, and the silver foil was rinsed to remove residual $^{35}SO_4^{2-}$. The reduced sulfate, which had precipitated as $Ag_2{}^{35}S$, was digitally mapped by using a BioRad Molecular Imager System GS-525 (Hercules, California) radioactive gel scanner. A similar technique was successfully used by Krumholz et al. (1997), who used Ag foil to map $^{35}S^{2-}$ produced by sulfate-reducing bacteria in subsurface rock samples.

As a complement to the foil incubations, quantitative measurements of sulfate-reduction rates in individual layers were made with conventional techniques. Subsamples of NS8a2 and NS11a were dissected into layers, as in Figure 1, and sulfate-reduction rates were determined by using $^{35}SO_4^{2-}$ (0.5 μCi sample; Ammersham, Chicago, Illinois) under both oxic and anoxic conditions (Visscher et al., 1998, 1999). Following 4–6 h of incubation with the radiolabel, sulfate reduction was assessed using the single-step chromium reduction method of Fossing and Jørgensen (1989). The rates were calculated by assuming 14 h of oxic conditions and 10 h of anoxia per 24 h (Visscher et al., 1998).

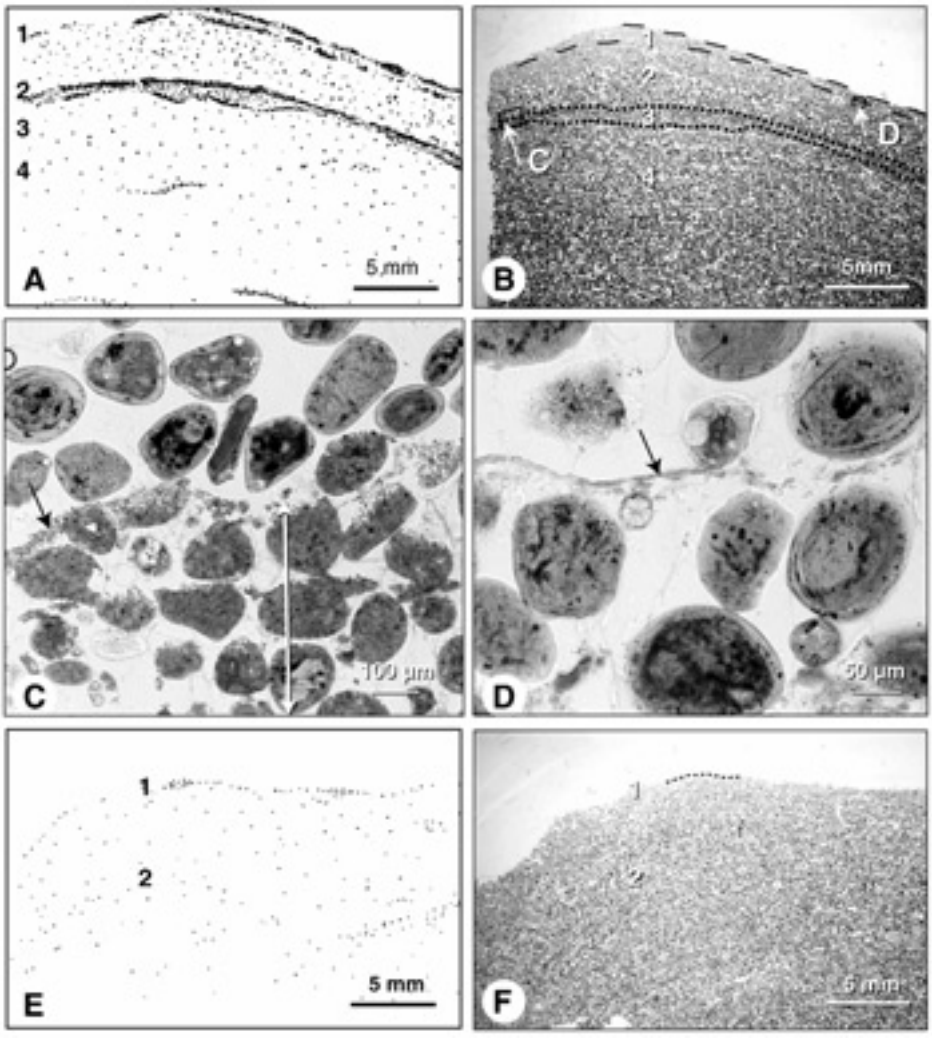

Figure 2. Comparison of sulfate-reduction (SR) activities, as mapped with Ag-foil technique, and microstructures, as observed in petrographic thin sections. A: Silver foil of mat NS8a2; density and size of black dots indicate locations and relative degree of SR activity. B: Low-magnification photomicrograph of thin-section NS8a2, composed mainly of fine-sand–sized carbonate grains. Dashed lines in layer 1 indicate thin crusts of micritic precipitate; dotted lines in layer 3 indicate top and bottom of lithified horizon of micritized grains. Boxes indicated by white arrows are shown in C and D. C: Higher magnification view of band of micritized grains in layer 3, panel B. White arrow indicates micritized zone, where grains have been altered by intense microboring; black arrow indicates micritic crust at top of micritized zone. D: Higher magnification view showing subsurface micritic crust (arrow) in layer 1, as indicated in panel B. E: Ag-foil of NS11a; smaller sizes and dispersed nature of dots, when compared to NS8a2 (panel A), indicate lower sulfate-reduction activity in this sample. F: Low-magnification photomicrograph of thin-section NS11a; dotted line along surface indicates poorly developed zone of micritized grains.

RESULTS

The distribution of reduced sulfate on the $^{35}SO_4^{2-}$-coated Ag foil, as indicated by the black dots ($Ag_2{}^{35}S$) in Figure 2 (A and E), shows the locations and relative activities of sulfate reduction. Mapping by this method enabled detection of sulfate-reducing activity with a resolution of tens of micrometers. In NS8a2, a double band of concentrated black dots along the surface of the mat (Fig. 2A) correlates with high sulfate-reducing activity in layer 1. The double band indicates, moreover, that there are two distinct zones of enhanced sulfate-reducing activity within this layer. A wider band of sulfate-reducing activity is also found at 3–4 mm depth, corresponding to layer 3; the upper and lower edges of this band show enhanced activity. In layers 2 and 4, dispersed but distinct black dots indicate moderate but diffuse sulfate-reducing activity. Sulfate-reducing activity is much lower in NS11a than in NS8a2, showing few features on the Ag foil (Fig. 2E). Two small areas on the surface of NS11a show slightly enhanced sulfate-reducing activity; nevertheless, as indicated by the low concentration and faint appearance of the black dots, most of this sample shows extremely low sulfate-reducing activity (Fig. 2E). When the distribution of pixels on the foil for NS8a2 is assessed, layer 1 accounts for 33% of the total sulfate-reducing activity, layer 2 for 11%, layer 3 for 44%, and layer 4 for 11%. Similar calculations for NS11a show that 40% of the sulfate-reducing activity is associated with layer 1 and 60% with layer 2. This distribution is affected by the thickness of the various layers.

Petrographic thin sections corresponding to the mat surfaces mapped by the Ag-foil technique display characteristic microstructures. Two

bands of thin micritic crust are present near the top of NS8a2, within layer 1 (Fig. 2B and 2D). These crusts are 10–40 μm thick and bridge carbonate grains. In addition, layer 3 in NS8a2, which was crusty in hand sample, is a band of micritized grains (Fig. 2B and 2C); micritic crusts show patchy development along the top (Fig. 2C) and bottom of this micritized band. In contrast to NS8a2, micritic crusts and micritized horizons are absent in NS11a, except for a single patch of weakly developed micritized grains on the top surface of layer 1 (Fig. 2F).

The conventional sulfate-reduction rate measurements using $^{35}SO_4^{2-}$ show activity patterns comparable to those detected with the Ag foils (Fig. 3). These radioisotope analyses indicate that the sulfate-reduction rate (and consequently activity) of NS8a2 appears higher in lithified layer 1 than in adjacent unlithified layer layer 2 and, similarly, higher in layer 3 than in adjacent layers 2 and 4 (Fig. 3, left panel). A significant rate in layer 1 of NS8a2 persists during the daytime (10.2 μ*M* SO_4^{2-} per hour) despite the presence of O_2 at the surface of the mat. The surface layer of NS11a shows a higher rate than layer 2 (Fig. 3, right panel). SR rates in NS8a2 are, however, 2–5 times higher than in NS11a, and when calculated per unit surface area for the top 8 mm, the rates are 438 and 102 nmol·cm^{-2}·d^{-1}, respectively, for NS8a2 and NS11a.

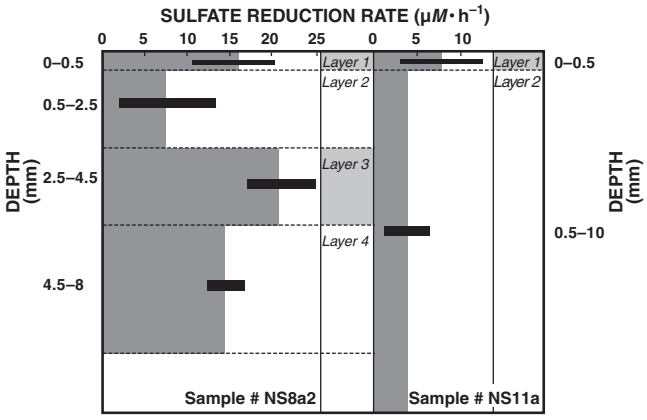

Figure 3. Vertical profiles of sulfate-reduction rates in stromatolite samples NS8a2 (left panel) and NS11a (right panel), of Highborne Cay, Bahamas. Rates were determined in separate layers through $^{35}SO_4^{2-}$ incubation. Approximate thickness of layers is indicated by width of horizontal panels. Rates presented combine oxic and anoxic measurements in replicate samples. Error bars indicate standard deviation.

DISCUSSION AND CONCLUSIONS

Our results demonstrate a direct correlation between sulfate-reducing activity, as indicated by the Ag foils (Fig. 2A and 2E), and lithified micritic horizons, as observed in petrographic thin sections (Fig. 2B and 2F). The two micritic crusts in layer 1 of NS8a2 (Fig. 2B) coincide with the double band of high sulfate-reducing activity in this layer (Fig. 2A). In addition, the band of micritized grains that composes layer 3 of NS8a2 (Fig. 2B and 2C) also coincides with a band of increased sulfate-reducing activity (Fig. 2A). It is notable that sulfate reduction is higher at the top and bottom of layer 3 than in the middle; these areas of increased sulfate-reducing activity probably correspond to the presence of micritic crusts, which show patchy development along these horizons. In contrast, distinct micritic horizons are not present in NS11a (Fig. 2F), and this sample shows weak sulfate-reducing activity (Fig. 2E). The patch of weakly micritized grains at the top of NS11a (Fig. 2F) is, nonetheless, a zone of slightly increased sulfate-reducing activity.

Micritic crusts and layers of micritized grains forming lithified laminae are characteristic features of Exuma stromatolites. Previous studies have shown that the micritized layers are zones of intense microboring by the endolithic cyanobacterium, *Solentia* sp. (Macintyre et al., 2000). Micrite precipitates in the boreholes coincident with the microboring activity; moreover, as *Solentia* crosses between grain boundaries, adjacent grains are welded together to form a framework structure (Macintyre et al., 2000). These micritized layers thus provide major structural support for the stromatolites. The micritic crusts, in contrast, are very thin; although they are cohesive enough to bridge grains (Fig. 2D), they are not major structural features. Note, for example, that layer 1 of NS8a2 appears soft in hand sample, even though it contains two micritic crusts. It is, however, significant to note that the micritic crusts are similar in thickness to micritic laminae in many ancient stromatolites, which are commonly 10–60 μm thick (Bertrand-Sarfati, 1976; Walter, 1983). It is therefore possible that processes of precipitation-forming micritic crusts in modern marine stromatolites could have been important in the formation of these fossilized structures.

The close coupling of sulfate reduction and microstructure in samples NS8a2 and NS11a is evidence that microbial sulfate reduction is an important mechanism of carbonate precipitation that forms lithified micritic layers in the Exuma stromatolites. Although other types of microbial activity may contribute to the formation of micritic laminae, sulfate reduction is arguably the dominant process. Major functional groups of bacteria in microbial mats include cyanobacteria, aerobic heterotrophic bacteria, sulfate-reducing bacteria, and sulfide-oxidizing bacteria (Visscher and Van Gemerden, 1993; Van Gemerden, 1993). $CaCO_3$ may precipitate through cyanobacterial oxygenic photosynthesis (PS) and could dissolve during aerobic heterotrophic respiration (AR). Uncoupling of PS and AR may result in net calcium carbonate precipitation or dissolution (Pinckney et al., 1995). However, PS and AR are usually coupled: during daytime, PS produces O_2 and fixed carbon, while AR requires O_2 and carbon. Both processes are limited to daytime, because PS is driven by light energy and at night O_2 is typically not present below ~0.5 mm depth in the mat (Visscher et al., 1998). Sulfate reduction is an alternative form of respiration and peaks at night, when O_2 is absent (Visscher et al., 1998, 1999). In addition, it is well known that sulfate reduction also occurs in the presence of O_2 (Canfield and Des Marais, 1991; Fründ and Cohen, 1992; Visscher et al., 1992; Jørgensen, 1994), albeit at lower rates (e.g., in NS8a2 10.2 μ*M*·h^{-1} vs. 18.5 μ*M*·h^{-1}, with and without O_2, respectively). HS^-, a product of sulfate reduction, is reoxidized during microbial sulfide oxidation, a process that results in $CaCO_3$ dissolution (Visscher et al., 1998):

$$HS^- + 2O_2 + CaCO_3 \rightarrow SO_4^{2-} + HCO_3^- + Ca^{2+}.$$

Typically, sulfide oxidation by chemosynthetic sulfur bacteria requires O_2 (Kelly, 1982) and is therefore largely absent during the night. HS^- produced during the night likely diffuses upward and out of the stromatolite. As a result, sulfate reduction and sulfide oxidation are more likely to be uncoupled in time and space than PS and AR. There are, therefore, compelling geomicrobial grounds to attribute $CaCO_3$ precipitation primarily to sulfate-reducing activity. *Schizothrix* also plays a key role in this scenario, because its in situ production of small organic carbon compounds and exopolymer fuels heterotrophic activity. Remnants of exopolymer that persist below the depth of active cyanobacterial growth can be used as an organic carbon source for bacteria such as sulfate-reducing bacteria (Visscher et al., 1999). In addition, *Solentia* may provide fixed organic carbon for sulfate-reducing activity in the gray, crusty layers (e.g., layer 3 of NS8a2). It is conceivable that sulfate-reducing bacteria are involved with carbonate precipitation within the endolithic boreholes.

Microorganisms facilitate $CaCO_3$ precipitation by changing the pCO_2 through their metabolism, as already outlined. In addition, they create a favorable chemical microenvironment for carbonate precipitation by active excretion of Ca^{2+}, which is toxic for the cell at seawater concentrations (Kempe and Kazmierczak, 1994). In addition, Ca^{2+} bound by polymer carboxyl groups is liberated during exopolymer degradation (Decho, 1990). Both increased pCO_2 and released Ca^{2+} favor $CaCO_3$ precipitation. It is interesting that bacteria actually benefit from carbonate precipitation on their surfaces, because this gener-

ates protons on the outside of the cell membrane (McConnaughey and Whelan, 1997):

$$Ca^{2+} + HCO_3^- \rightarrow CaCO_3 + H^+.$$

The proton gradient thus created across the bacterial cell membrane, or proton motive force, presents the basic energy currency that drives, e.g., ATP formation, substrate uptake, and flagella (Nicholls and Ferguson, 1992).

Grotzinger and Knoll (1999) attributed cementation in stromatolites to abiotic, inorganic processes and referred to lithified layers as marine cement. In contrast, our work shows compelling evidence of biological-controlled formation of micritic laminae. Furthermore, our current study stresses the need to better understand coupling of microstructure and microbial processes. Microscale observations of biological activity, such as those provided by the Ag-foil technique, are indispensable for elucidating the origin of microstructure in stromatolites.

ACKNOWLEDGMENTS

This work was supported by National Science Foundations grants OCE-9619314 (to Visscher) and OCE-9530215 (to Reid). We thank Y. Cohen for sharing details of the Ag-foil technique, Don Dean, Smithsonian Institution, for making the petrographic thin sections, and Meg Coleman and Dan Rogers for reading the manuscript. This is Research Initiative in Bahamian Stromatolites (RIBS) contribution 9.

REFERENCES CITED

Abd-El-Malek, Y., and Rizk, S.G., 1963, Bacterial sulfate reduction and the development of alkalinity: III. Experiments under natural conditions in the Wadi Natrun: Journal of Applied Bacteriology, v. 26, p. 20–26.

Baas Becking, L.G.M., 1934, Geobiologie: The Hague, W.P. Stockum & Zoon, 263 p.

Bertrand-Sarfati, J., 1976, An attempt to classify late Precambrian stromatolite microstructures, *in* Walter, M.R., ed., Stromatolites: New York, Elsevier, p. 251–259.

Buczynski, C., and Chafetz, H.S., 1991, Habits of bacterially induced precipitates of calcium carbonate and the influence of medium viscosity on mineralogy: Journal of Sedimentary Petrology, v. 61, p. 226–233.

Canfield, D.E., and Des Marais, D.J., 1991, Aerobic sulfate reduction in microbial mats: Science, v. 251, p. 1471–1473.

Cohen, Y., 1984, Comparative N and S cycles: Oxygenic photosynthesis, anoxygenic photosynthesis, and sulfate-reduction in cyanobacterial mats, *in* Klug, M.J., and Reddy, C.A., eds., Recent advances in microbial ecology: Washington, D.C., American Society for Microbiology Press, p. 435–441.

Cohen, Y., and Helman, Y., 1997, Two-dimensional sub-millimetric mapping of sulfate reduction in marine sediments: American Society for Microbiology 97th General Meeting, Miami Beach, Florida, Abstracts, p. 393.

Decho, A.W., 1990, Microbial exopolymer secretions in oceanic environments: Their role(s) in food webs and marine processes: Oceanography and Marine Biology Annual Review, v. 28, p. 73–154.

Des Marais, D.J., 1990, Microbial mats and the early evolution of life: Trends in Ecology and Evolution, v. 5, p. 140–145.

Dill, R.F., Shinn, E.A., Jones, A.T., Kelly, K., and Steinen, R.P., 1986, Giant subtidal stromatolites forming in normal salinity water: Nature, v. 324, p. 55–58.

Feldmann, M., and Mackenzie, J., 1998, Stromatolite-thrombolite association in a modern environment, Lee Stocking Island, Bahamas: Palaios, v. 13, p. 201–212.

Fossing, H., and Jørgensen, B.B., 1989, Measurement of bacterial sulfate reduction in sediments: Evaluation of a single-step chromium reduction method: Biogeochemistry, v. 8, p. 205–222.

Froelich, P.N., Klinkhammer, G.P., Bender, M.L., Luedtke, N.A., Heath, G.R., Cullen, D., and Dauphin, P., 1979, Early oxidation of organic matter in pelagic sediments of the eastern equatorial Atlantic: Suboxic diagenesis: Geochimica et Cosmochimica Acta, v. 43, p. 1075–1090.

Fründ, C., and Cohen, Y., 1992, Diurnal cycles of sulfate reduction under oxic conditions in microbial mats: Applied and Environmental Microbiology, v. 58, p. 70–77.

Golubic, S., and Browne, K., 1996, *Schizothrix gebeleinii* sp. Nova builds subtidal stromatolites, Lee Stocking Island, Bahamas: Algological Studies, v. 83, p. 273–290.

Grotzinger, J.P., and Knoll, A.H., 1999, Stromatolites in Precambrian carbonates: Evolutionary mileposts or environmental dipsticks?: Annual Review of Earth and Planetary Sciences, v. 27, p. 313–358.

Jørgensen, B.B., 1994, Sulfate reduction and thiosulfate transformation in a cyanobacterial mat during a diel oxygen cycle: FEMS Microbiology Ecology, v. 13, p. 303–312.

Jørgensen, B.B., and Cohen, Y., 1977, Solar Lake (Sinai): 5. The sulfur cycle of the benthic cyanobacterial mat: Limnology and Oceanography, v. 22, p. 657–666.

Kazmierczak, J., and Kempe, S., 1990, Modern cyanobacterial analogs of Paleozoic stromatoporoids: Science, v. 250, p. 1244–1248.

Kelly, D.P., 1982, Biochemistry of the chemolithotrophic oxidation of inorganic sulphur: Royal Society of London Philosophical Transactions, ser. B., v. 298, p. 499–528.

Kempe, S., and Kazmierczak, J., 1994, The role of alkalinity in the evolution of ocean chemistry, organization of living systems and biocalcification processes: Bulletin de l'Institut Oceanographique Monaco, v. 13, p. 61–117.

Krumbein, W.E., Cohen, Y., and Shilo, M., 1977, Solar Lake (Sinai): 4. Stromatolitic cyanobacterial mats: Limnology and Oceanography, v. 22, p. 635–656.

Krumholz, L.R., McKinley, J.P., Ulrich, G.A., and Suflita, J.M., 1997, Confined subsurface microbial communities in Cretaceous rock: Nature, v. 386, p. 64–66.

Lyons, W.B., Long, D.T., Hines, M.E., Gaudette, H.E., and Armstrong, P.B., 1984, Calcification of cyanobacterial mats in Solar Lake, Sinai: Geology, v. 12, p. 623–626.

Macintyre, I.G., Reid, R.P., and Steneck, R.S., 1996, Growth history of stromatolites in a Holocene fringing reef, Stocking Island, Bahamas: Journal of Sedimentary Research, v. 66, p. 231–242.

Macintyre, I.G., Pufert-Bebout, L., and Reid, R.P., 2000, The role of endolithic cyanobacteria in the formation of lithified laminae in Bahamian stromatolites: Journal of Sedimentary Research (in press).

McConnaughey, T.A., and Whelan, J.F., 1997, Calcification generates protons for nutrient and bicarbonate uptake: Earth Sciences Reviews, v. 42, p. 95–117.

Nicholls, D.G., and Ferguson, S.J., 1992, Bioenergetics 2: London, Academic Press, 255 p.

Pinckney, J., Paerl, H.W., Reid, R.P., and Bebout, B.M., 1995, Ecophysiology of stromatolitic mats, Stocking Island, Exuma Cays, Bahamas: Microbial Ecology, v. 29, p. 19–37.

Reid, R.P., Macintyre, I.G., Browne, K.M., Steneck, R.S., and Miller, T., 1995, Modern marine stromatolites in the Exuma Cays, Bahamas: Uncommonly common: Facies, v. 33, p. 1–18.

Reid, R.P., Macintyre, I.G., and Steneck, R.S., 1999, A microbialite/algal-ridge fringing reef complex, Highborne Cay, Bahamas: Atoll Research Bulletin 465, 18 p.

Thompson, J.B., and Ferris, F.G., 1990, Cyanobacterial precipitation of gypsum, calcite, and magnesite from natural alkaline lake water: Geology, v. 18, p. 995–998.

Van Gemerden, H., 1993, Microbial mats: A joint venture: Marine Geology, v. 113, p. 3–25.

Vasconcelos, C., Mackenzie, J.A., Bernasconi, S., Grujic, D., and Tien, A.J., 1995, Microbial mediation as a possible mechanism for natural dolomite formation at low temperatures: Nature, v. 377, p. 220–222.

Visscher, P.T., and van Gemerden, H., 1993, Sulfur cycling in laminated marine microbial ecosystems, *in* Oremland, R.S., ed., Biogeochemistry of global change: New York, Chapman and Hall, p. 672–690.

Visscher, P.T., Prins, R.A., and van Gemerden, H., 1992, Rates of sulfate reduction and thiosulfate consumption in a marine microbial mat: FEMS Microbiology Ecology, v. 86, p. 283–394.

Visscher, P.T., Reid, R.P., Bebout, B.M., Hoeft, S.E., Macintyre, I.G., and Thompson, J.A., Jr., 1998, Formation of lithified micritic laminae in modern marine stromatolites (Bahamas): The role of sulfur cycling: American Mineralogist, v. 83, p. 1482–1493.

Visscher, P.T., Gritzer, R.F., and Leadbetter, E.R., 1999, Low-molecular-weight sulfonates, a major substrate for sulfate reducers in marine microbial mats: Applied and Environmental Microbiology, v. 65, p. 3272–3278.

Walter, L.M., Bischof, S.A., Patterson, W.P., and Lyons, T.W., 1993, Dissolution and recrystallization in modern shelf carbonates: Evidence from pore water and solid phase chemistry: Royal Society of London Philosophical Transactions, ser. A., v. 344, p. 27–36.

Walter, M.R., 1983, Archean stromatolites: Evidence of the Earth's earliest benthos, *in* Schopf, J.W., ed., Earth's earliest biosphere, its origin and evolution: Princeton, New Jersey, Princeton University Press, p. 187–213.

Manuscript received December 13, 1999
Revised manuscript received June 21, 2000
Manuscript accepted July 19, 2000